Opto- and electro-mechanical entanglement improved by modulation

2012 New J. Phys. 14 075014

(http://iopscience.iop.org/1367-2630/14/7/075014)

New Journal of Physics
The open-access journal for physics

Opto- and electro-mechanical entanglement improved by modulation

A Mari[1,2] **and J Eisert**[1,2,3]

[1] Dahlem Center for Complex Quantum Systems, Freie Universität Berlin, 14195 Berlin, Germany
[2] Institute of Physics and Astronomy, University of Potsdam, D-14476 Potsdam, Germany
E-mail: jense@physik.fu-berlin.de

New Journal of Physics **14** (2012) 075014 (12pp)
Received 7 February 2012
Published 19 July 2012
Online at http://www.njp.org/
doi:10.1088/1367-2630/14/7/075014

Abstract. One of the main milestones in the study of opto- and electro-mechanical systems is to certify entanglement between a mechanical resonator and an optical or microwave mode of a cavity field. In this work, we show how a suitable time-periodic modulation can help to achieve large degrees of entanglement, building upon the framework introduced in Mari and Eisert (2009 *Phys. Rev. Lett.* **103** 213603). It is demonstrated that with suitable driving, the maximum degree of entanglement can be significantly enhanced, in a way exhibiting a nontrivial dependence on the specifics of the modulation. Such time-dependent driving might help to experimentally achieve entangled mechanical systems also in situations when quantum correlations are otherwise suppressed by thermal noise.

[3] Author to whom any correspondence should be addressed.

Contents

1. Introduction

Opto-mechanical [1–7] and electro-mechanical systems [8–13] are promising candidates for realizing architectures exhibiting quantum behavior in macroscopic structures. Once the quantum regime is reached, exciting applications in quantum technologies such as realizing precise force sensors are conceivable [15, 16]. One of the requirements to render such an approach feasible, needless to say, is to be able to certify that a mechanical degree of freedom is deeply in the quantum regime [16–20]. The detection of entanglement arguably constitutes the ultimate benchmark in this respect. While effective ground state cooling has indeed been closely approached experimentally [6, 10] and achieved [7, 9, 13], the detection of entanglement is still in progress.

In this paper, we emphasize that a mere suitable time modulation of the driving field may significantly help to achieve entanglement between a mechanical mode and a radiation mode of the system. We extend the idea of [21], putting emphasis on the improvement of entanglement by means of suitable modulations [21–23]. This time dependence of the driving indirectly affects the effective radiation pressure coupling between the two modes and generates non-trivial entanglement resonances. In comparison with single-mode squeezing, which is the main subject of [21], here we show that two-mode squeezing is optimized at different modulation frequencies related to the normal mode splitting of the system.

Several other schemes have been proposed in the literature for squeezing or entangling a mechanical mode with an optical or microwave field. These are based on driving one single sideband [14, 19, 20, 30], driving two sidebands with the same power [23], driving two independent modes of the cavity [29] and directly modulating the frequencies of the modes (parametric amplification) [22]. In our system, a single cavity mode is externally driven with a red-detuned main carrier and modulated with a weak blue sideband tuned at particular resonance frequencies. In this way, the system is stable and with the appropriate choice of the driving pattern, large degrees of two-mode squeezing can be reached. Moreover, in our scheme, entanglement appears in the long time limit as a stationary property without the need for any post-selection of the state conditioned on external measurement results.

The body of the paper is organized into four sections. In the first two sections the classical dynamics of the system and its quantum fluctuations are studied in a very general framework.

In the third section, we focus on the main result of the paper: the appearance of entanglement resonances for particular choices of the modulation frequencies. In section 4, this resonance phenomenon is applied to two examples of opto- and electro-mechanical systems, whose parameters have been realistically chosen in agreement with recent experiments.

2. Modulated opto- and electro-mechanical systems

We consider the simplest scenario of a mechanical resonator of frequency $\omega_{\rm m}$ coupled to a single mode of the electromagnetic field of frequency ω_a. This radiation field could be an optical mode of a Fabry–Perot cavity [1–7, 18, 19, 24] or a microwave mode of a superconductive circuit [8–10, 14]. It can be shown that the Hamiltonians associated with this two experimental settings are formally equivalent [14, 19] and therefore the theory that we are going to introduce is general enough to describe both types of systems.

We assume that the radiation mode is driven by a coherent field with a time-dependent amplitude $E(t)$ and frequency ω_l. The particular choice of the time dependence is left unspecified but we impose the structure of a periodic modulation such that $E(t+\tau)=E(t)$ for some $\tau>0$ of the order of ω_m^{-1}. In this sense, the driving regime that we are going to study is intermediate between the two opposite extremes of constant amplitude and short pulses. The Hamiltonian of the system is

$$H=\hbar\omega_a a^\dagger a+\tfrac{1}{2}\hbar\omega_m(p^2+q^2)-\hbar g a^\dagger a q+\mathrm{i}\hbar[E(t)\mathrm{e}^{-\mathrm{i}\omega_l t}a^\dagger-E^*(t)\mathrm{e}^{\mathrm{i}\omega_l t}a], \qquad (1)$$

where the mechanical mode is described in terms of dimensionless position and momentum operators satisfying $[q,\,p]=i$, while the radiation mode is captured by creation and annihilation operators obeying the bosonic commutation rule $[a,a^\dagger]=1$. The two modes interact via a radiation pressure potential with a strength given by the coupling parameter g.

In addition to this coherent dynamics, the mechanical mode will be unavoidably damped at a rate $\gamma_{\rm m}$, while the optical/microwave mode will decay at a rate κ. These dissipative processes and the associated fluctuations can be taken into account in the Heisenberg picture by the following set of quantum Langevin equations [14, 17–19]:

$$\begin{aligned}\dot q &=\omega_{\rm m}p,\\ \dot p &=-\omega_{\rm m}q-\gamma_m p+g a^\dagger a+\xi,\\ \dot a &=-(\kappa+\mathrm{i}\Delta)a+igaq+E(t)+\sqrt{2\kappa}a^{\rm in}.\end{aligned} \qquad (2)$$

In this set of equations a convenient rotating frame has been chosen $a\mapsto a\,\mathrm{e}^{-\mathrm{i}\omega_l t}$, such that the detuning parameter is $\Delta=\omega_a-\omega_l$. The operators ξ and $a^{\rm in}$ represent the mechanical and optical bath operators respectively, and their correlation functions are well approximated by delta functions

$$\begin{aligned}&\langle\xi(t)\xi(t')+\xi(t')\xi(t)\rangle/2=\gamma_m(2n_m+1)\delta(t-t'),\\ &\langle a^{\rm in}(t)a^{\rm in\dagger}(t')\rangle=(n_a+1)\delta(t-t'),\\ &\langle a^{\rm in\dagger}(t)a^{\rm in}(t')\rangle=n_a\delta(t-t'),\end{aligned} \qquad (3)$$

where $n_x=(\exp(\hbar\omega_x/(k_BT))-1)^{-1}$, is the bosonic mean occupation number at temperature T.

3. Classical periodic orbits: first moments

We are interested in the coherent strong driving regime when $\langle a\rangle \gg 1$. In this limit, the semiclassical approximations $\langle a^\dagger a\rangle \simeq |\langle a\rangle|^2$ and $\langle aq\rangle \simeq \langle a\rangle\langle q\rangle$ are good approximations. Within this approximation, one can average both sides of equation (2) and get a differential equation for the first moments of the canonical coordinates

$$\begin{aligned}\langle\dot{q}\rangle &= \omega_{\rm m}\langle p\rangle,\\ \langle\dot{p}\rangle &= -\omega_{\rm m}\langle q\rangle - \gamma_{\rm m}\langle p\rangle + g|\langle a\rangle|^2,\\ \langle\dot{a}\rangle &= -(\kappa + {\rm i}\Delta)\langle a\rangle + {\rm i}g\langle a\rangle\langle q\rangle + E(t).\end{aligned} \tag{4}$$

Far away from the well known opto- and electro-mechanical instabilities, asymptotic τ-periodic solutions can be used as ansätze for equation (4) (see the appendix for a more detailed analysis). These solutions represent periodic orbits in phase space and are usually called the limit cycles. These cycles are induced by modulation and should not be confused with the limit cycles emerging in the strong driving regime due to the nonlinearity of the system. Because of the asymptotic periodicity of the solutions, one can define the fundamental modulation frequency as $\Omega = 2\pi/\tau$, such that each periodic solution can be expanded in the following Fourier series

$$\langle O(t)\rangle = \sum_{n=-\infty}^{\infty} O_n\, {\rm e}^{{\rm i}n\Omega t}, \quad O = q,\, p,\, a. \tag{5}$$

The Fourier coefficients $\{O_n\}$ appearing in equation (5) can be analytically estimated as shown in the appendix and they completely characterize the classical asymptotic dynamics of the system.

Finally we note that the classical evolution of the dynamical variables will shift the detuning to the effective value of $\tilde{\Delta}(t) = \Delta - g\langle q(t)\rangle$. For the same reason, it is also convenient to introduce an effective coupling constant defined as

$$\tilde{g}(t) = \sqrt{2}g\langle a(t)\rangle. \tag{6}$$

4. Quantum correlations: second moments

The classical limit cycles are given by the asymptotic solutions of equation (4). In order to capture the quantum fluctuations around the classical orbits, we introduce a column vector of new quadrature operators $u = [\delta q, \delta p, \delta x, \delta y]^{\rm T}$ defined as:

$$\begin{aligned}\delta q &= q - \langle q(t)\rangle,\\ \delta p &= p - \langle p(t)\rangle,\\ \delta x &= \left[(a - \langle a(t)\rangle) + (a - \langle a(t)\rangle)^\dagger\right]/\sqrt{2},\\ \delta y &= -{\rm i}\left[(a - \langle a(t)\rangle) - (a - \langle a(t)\rangle)^\dagger\right]/\sqrt{2}.\end{aligned} \tag{7}$$

This set of canonical coordinates can be viewed as describing a time-dependent reference frame co-moving with the classical orbits. The corresponding vector of noise operators will be

$$n = [0, \xi, (a^{\rm in} + a^{{\rm in}\dagger})/\sqrt{2}, -{\rm i}(a^{\rm in} - a^{{\rm in}\dagger})/\sqrt{2}]^{\rm T}. \tag{8}$$

Since we are in the limit in which classical orbits emerge ($\langle a\rangle \gg 1$), it is a reasonable approximation to express the previous set of Langevin equations (2) in terms of the new fluctuation operators (7) and neglect all their quadratic powers. The resulting linearized system can be written as a matrix equation [21],

$$\dot{u} = A(t)u + n(t), \tag{9}$$

where

$$A(t) = \begin{bmatrix} 0 & \omega_{\rm m} & 0 & 0 \\ -\omega_{\rm m} & -\gamma_{\rm m} & \Re\tilde{g}(t) & \Im\tilde{g}(t) \\ -\Im\tilde{g}(t) & 0 & -\kappa & \tilde{\Delta}(t) \\ \Re\tilde{g}(t) & 0 & -\tilde{\Delta}(t) & -\kappa \end{bmatrix} \tag{10}$$

is a real time-dependent matrix.

If the system is stable, and as long as the linearization is valid, the quantum state of the system will converge to a Gaussian state with time-dependent first and second moments. The first moments of the state correspond to the classical limit cycles introduced in the previous section. The second moments can be expressed in terms of the covariance matrix $V(t)$ with entries

$$V_{k,l}(t) = \langle u_k(t)u_l^{\dagger}(t) + u_l^{\dagger}(t)u_k(t)\rangle/2. \tag{11}$$

One can also define a diffusion matrix D as

$$\delta(t-t')D_{k,l} = \langle n_k(t)n_l^{\dagger}(t') + n_l^{\dagger}(t')n_k(t)\rangle/2, \tag{12}$$

which, from the properties of the bath operators (4), is diagonal and equal to

$$D = \mathrm{diag}[0, \gamma(2n_m+1), \kappa(2n_a+1), \kappa(2n_a+1)]. \tag{13}$$

From equations (9) and (12), one can easily derive a linear differential equation for the correlation matrix,

$$\frac{\mathrm{d}}{\mathrm{d}t}V(t) = A(t)V(t) + V(t)A^{\mathrm{T}}(t) + D. \tag{14}$$

Since the first and second moments are specified, equations (4) and (14) provide a complete description of the asymptotic dynamics of the system. Apart from the linearization around classical cycles, no further approximation has been done: neither a weak coupling, adiabatic non rotating-wave approximation. Numerical solutions of both equations (4) and (14) can be straightforwardly found. These solutions will be used to calculate the exact amount of opto- and electro-mechanical entanglement present in the system.

The asymptotic periodicity of the classical solutions (equation (5)) implies that, in the long time limit, $A(t+\tau) = A(t)$. This means that equation (14) is a linear differential equation with periodic coefficients and then all the machinery of Floquet theory is in principle applicable. Here, however, since we are only interested in asymptotic solutions, we are not going to study all the Floquet exponents of the system. The only property that we need is that, in the long time limit, stable solutions will acquire the same periodicity of the coefficients:

$$V(t+\tau) = V(t). \tag{15}$$

This is a simple corollary of Floquet's theorem. In the subsequent sections we will apply the previous theory to some particular experimental setting and show how a simple modulation of the driving field can significantly improve the amount of opto- and electro-mechanical entanglement.

5. Entanglement resonances

In this section, we are going to study what kind of amplitude modulation is optimal for generating entanglement between the radiation and mechanical modes. As a measure of entanglement we use the logarithmic negativity $E_{\rm N}$ which, since the state is Gaussian, can be easily computed directly from the correlation matrix $V(t)$ [26–28]. We have also seen that the correlation matrix is, in the long time limit, τ-periodic. This suggests that it is sufficient to study the variation of entanglement in a finite interval of time $[t, t+\tau]$ for large times t. One can then define the maximum amount of achievable entanglement as

$$\hat{E}_{\rm N} = \lim_{t\to\infty} \max_{h\in[t,t+\tau]} E_{\rm N}(h). \tag{16}$$

This will be the quantity that we are going to optimize.

We first study a very simple set of parameters (see caption of figure 1) in order to understand what the optimal choice is for the modulation frequency. For this purpose, we impose effective coupling to have this simple structure

$$\tilde{g}(t) = \tilde{g}_0 + \tilde{g}_\Omega\, {\rm e}^{-{\rm i}\Omega t}, \tag{17}$$

where $\tilde{g}_0$ is associated with the main driving field with detuning Δ, while $\tilde{g}_\Omega$ is the amplitude of a further sideband shifted by a frequency Ω from the main carrier. Without loss of generality we will assume $\tilde{g}_0$ and $\tilde{g}_\Omega$ to be positive reals. This kind of driving is a natural one and it has been chosen for reasons that will become clear later. From now on we set the detuning of the carrier frequency to be equal to the mechanical frequency $\Delta = \omega_{\rm m}$. This choice of the detuning corresponds to the well-known sideband cooling setting [17, 24] and it has been shown to be also optimal for maximizing opto-mechanical entanglement with a non-modulated driving [19]. Figure 1 shows the maximum entanglement $\hat{E}_{\rm N}$ between the mechanical and the radiation modes as a function of the modulation frequency Ω and for different values of the driving amplitude $\tilde{g}_0$. This maximum degree of entanglement has been calculated for $t > 200/\kappa$, when the system has well reached its periodic steady state.

We observe that in figure 1 there are two main resonant peaks at the modulation frequencies

$$\Omega \simeq 2\omega_{\rm m} \pm \tilde{g}_0, \tag{18}$$

that we are going to carefully explain later. Note also that, if compared to [21], the choices of modulations that give rise to the optimal local single-mode squeezing of the mechanical mode ($\Omega = 2\omega_{\rm m}$) and the degree of entanglement ($\Omega = 2\omega_{\rm m} \pm \tilde{g}_0$) are not identical. This is rooted in the 'monogamous nature' of squeezing: For a fixed spectrum of the covariance matrix, one can either have large local or two-mode squeezing. In figure 1 we also observe that the height of the two peaks, due to cavity filtering, is not equal: the first resonance at $\Omega = 2\omega_{\rm m} - \tilde{g}_0$ is better for the amount of steady state entanglement. One could also ask what the behavior of entanglement is when we change the amplitude of the modulation. Figure 2 shows the amount of entanglement $\hat{E}_{\rm N}$ as a function of $\tilde{g}_\Omega$ and for different choices of $\tilde{g}_0$. We observe that entanglement is monotonically increasing in $\tilde{g}_\Omega$ up to a threshold where the system becomes unstable.

We will now provide some intuition on why one should expect the main resonances at the locations where they are observed. The exact dynamics of the linearized system can be studied via equation (9). This is how figures 1 and 2 were generated. Now, however, we are going to

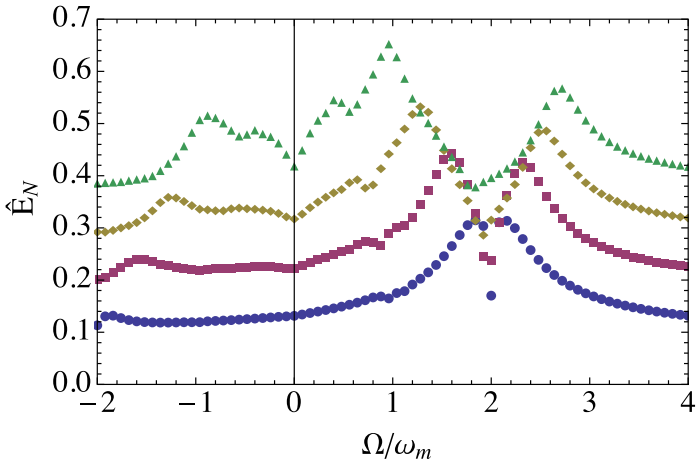

Figure 1. Maximum entanglement $\hat{E}_{\rm N}$ as a function of the modulation frequency Ω and for different values of the driving strength $\tilde{g}_0$. The chosen parameters in units of $\omega_{\rm m}$ are: $\kappa = 0.2$, $\gamma_{\rm m} = 10^{-6}$, $\tilde{\Delta} = 1$, $n_{\rm m} = n_a = 0$, $\tilde{g}_\Omega = 0.1$, $\tilde{g}_0 = 0.2$ (circles), 0.4 (squares), 0.6 (diamonds), 0.8 (triangles).

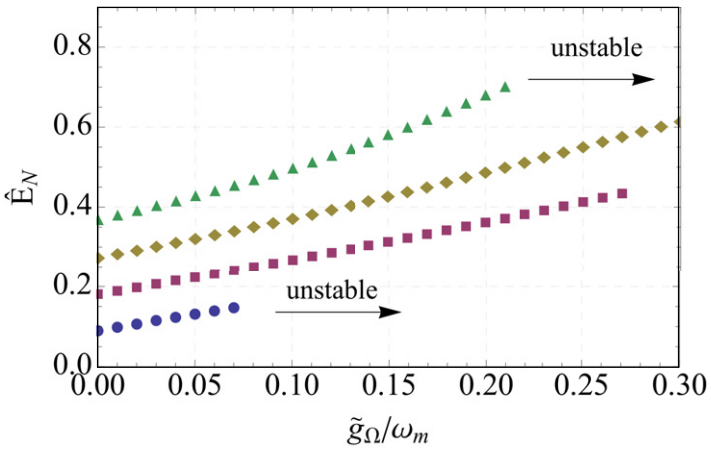

Figure 2. Maximum entanglement $\hat{E}_{\rm N}$ as a function of the modulation amplitude $\tilde{g}_\Omega$ and for different values of the driving strength $\tilde{g}_0$. The chosen parameters in units of $\omega_{\rm m}$ are: $\kappa = 0.2$, $\gamma_{\rm m} = 10^{-6}$, $\tilde{\Delta} = 1$, $n_{\rm m} = n_a = 0$, $\Omega = 2\omega_{\rm m} - \tilde{g}_0$, $\tilde{g}_0 = 0.2$ (circles), 0.4 (squares), 0.6 (diamonds), 0.8 (triangles). Beyond the ranges of parameters shown in this plot, i.e. for $\tilde{g}_0 \gtrsim 0.8$ and $\tilde{g}_\Omega \gtrsim 0.3$, the system is unstable.

make some strong approximations in order to better understand the physics of the problem. We rewrite the linearized Hamiltonian as a sum of three terms:

$$H = H_1 + H_2 + H_3, \tag{19}$$

$$H_1 = \hbar\Delta a^\dagger a + \hbar\omega_{\rm m} b^\dagger b, \tag{20}$$

$$H_2 = -\hbar\tilde{g}_0(a + a^\dagger)(b + b^\dagger)/2, \tag{21}$$

$$H_3 = -\hbar\tilde{g}_\Omega(e^{i\Omega t}a + e^{-i\Omega t}a^\dagger)(b + b^\dagger)/2, \tag{22}$$

where the new bosonic operators $a = (\delta x + \mathrm{i}\delta y)/\sqrt{2}$ and $b = (\delta q + \mathrm{i}\delta p)/\sqrt{2}$ are defined with respect to fluctuation quadratures. The three terms H_1, H_2 and H_3 correspond to free evolution, the driving carrier and the weak modulation sideband respectively. We assume the modulation term H_3 to be a weak 'perturbation of the perturbation' H_2. In other words we take two hierarchic limits $\omega \gg \tilde{g}_0 \gg \tilde{g}_\Omega$ that will allow us to perform two successive rotating wave approximations: first with respect to H_1 and then with respect to H_2. In interaction picture with respect to H_1 and remembering that we fixed $\Delta = \omega_\mathrm{m}$, we get:

$$H_2' \simeq -\hbar\tilde{g}_0(ab^\dagger + a^\dagger b)/2, \tag{23}$$

$$H_3' \simeq -\hbar\tilde{g}_\Omega(\mathrm{e}^{\mathrm{i}(\Omega-2\omega_\mathrm{m})t}ab + \mathrm{e}^{-\mathrm{i}(\Omega-2\omega_\mathrm{m})t}a^\dagger b^\dagger)/2. \tag{24}$$

In the first equation, we neglected all rotating terms while in the second we neglected the term proportional to $\mathrm{e}^{\mathrm{i}\Omega t}ab^\dagger + \mathrm{e}^{-\mathrm{i}\Omega t}a^\dagger b$ because it is resonant only in the trivial case of $\Omega = 0$ and produces only a renormalization of $\tilde{g}_0$. Now we apply the following Bogoliubov transformation

$$c_\pm = (a \pm b)/\sqrt{2}. \tag{25}$$

These new bosonic operators describe the well known hybridization of the system into normal modes as described in [5, 25]. In this canonical frame H_2' is diagonal and we get:

$$H_2' \simeq -\hbar\tilde{g}_\mathrm{o}(c_+^\dagger c_+ - c_-^\dagger c_-)/2, \tag{26}$$

$$H_3' \simeq -\hbar\tilde{g}_\Omega\,\mathrm{e}^{\mathrm{i}(\Omega-2\omega_\mathrm{m})t}(c_+c_+ + c_-c_-)/2 + \mathrm{h.c.} \tag{27}$$

We are finally ready to perform a second rotating wave approximation, which is valid in the weak modulation limit $\tilde{g}_0 \gg \tilde{g}_\Omega$. In interaction picture with respect to H_2' we obtain

$$H_3'' \simeq -\hbar\tilde{g}_\Omega\,\mathrm{e}^{\mathrm{i}(\Omega-2\omega_\mathrm{m})t}(\mathrm{e}^{\mathrm{i}\tilde{g}_0 t}c_+c_+ + \mathrm{e}^{-\mathrm{i}\tilde{g}_0 t}c_-c_-)/2 + \mathrm{h.c.} \tag{28}$$

From the structure of equation (28) we observe that there are two resonances $\Omega = 2\omega_\mathrm{m} \pm g$ associated with the two distinct squeezing interactions

$$H_\pm = -\hbar\tilde{g}_\Omega(c_\mp c_\mp + c_\mp^\dagger c_\mp^\dagger)/2. \tag{29}$$

Because of equation (25), squeezing of one of the hybrid modes implies that one of the Einstein–Podolsky–Rosen (EPR) variances is reduced below the uncertainty of the vacuum fluctuations. This suggests the presence of entanglement. Actually, bosonic modes with EPR correlations are the most relevant and paradigmatic example of entangled states and they are the basis of many quantum information protocols [26].

6. Opto- and electro-mechanical entanglement in realistic settings

We have seen that an effective coupling of the form $\tilde{g}(t) = \tilde{g}_0 + \tilde{g}_\Omega\,\mathrm{e}^{-\mathrm{i}(2\omega_\mathrm{m}-\tilde{g}_0)t}$ is optimal for the generation of entanglement within the considered class of drivings. However, the parameter $\tilde{g}(t)$ depends on the average amplitude $\langle a(t)\rangle$ and assuming such a simple structure may seem somewhat artificial. In this section, we show how the desired time-dependent coupling can indirectly result from the classical limit cycles of the system (see the insets of figures 3 and 4) and we also take into account the effect of a temperature of the order of $T \simeq 100\,\mathrm{mK}$. The natural 'educated guess' for the structure of the driving field will be

$$E(t) = E_0 + E_\Omega\,\mathrm{e}^{-\mathrm{i}(2\omega_\mathrm{m}-\tilde{g}_0)t}. \tag{30}$$

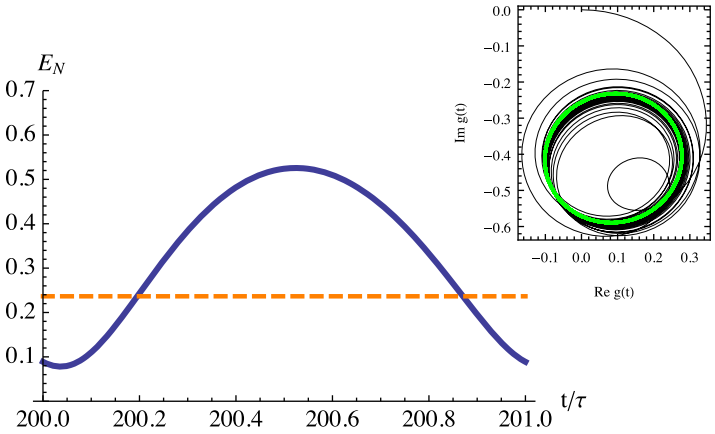

Figure 3. Optical cavity. The degree of entanglement, measured in terms of the logarithmic negativity, as a function of time. The full line refers to a modulated driving ($\Omega = 1.4\omega_{\rm m}$), whereas the dotted line corresponds to a non-modulated driving ($\Omega = 0$). The chosen parameters in units of $\omega_{\rm m}$ are: $\kappa = 0.2$, $\gamma_{\rm m} = 10^{-6}$, $\Delta = 1$, $n_{\rm m} = 2 \times 10^3$, $n_a = 0$, $g_0 = 4 \times 10^{-6}$, $E_0 = 7 \times 10^4$ and $E_\Omega = 2.5 \times 10^4$. The inset shows the trajectory of the effective coupling $\tilde{g}(t) = \sqrt{2}g\langle a(t)\rangle$ in the complex plane due to the time evolution of the optical amplitude. The phase-space orbit (black line) is numerically simulated from equation (4), while the limit cycle (green line) is an analytical approximation (see the appendix for more details).

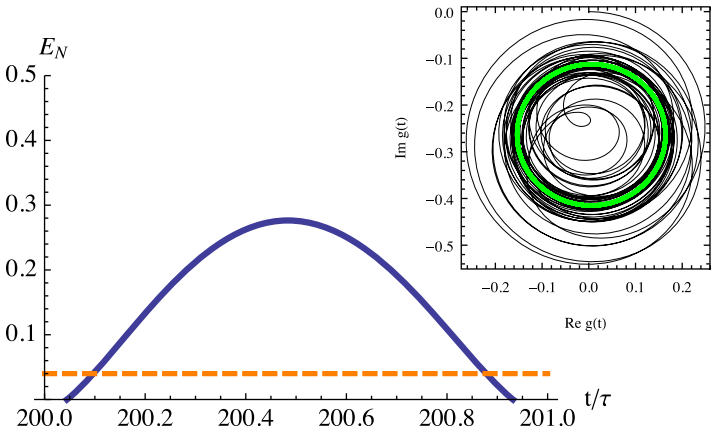

Figure 4. Microwave cavity. Entanglement log-negativity as a function of time. The full line refers to a modulated driving ($\Omega = 1.3\omega_{\rm m}$) whereas the dotted line corresponds to a non-modulated driving ($\Omega = 0$). The chosen parameters in units of $\omega_{\rm m}$ are: $\kappa = 0.02$, $\gamma_{\rm m} = 3 \times 10^{-6}$, $\Delta = 1$, $n_{\rm m} = 200$, $n_a = 0.03$, $g_0 = 2 \times 10^{-5}$, $E_0 = 9 \times 10^3$ and $E_\Omega = 1.3 \times 10^3$. The inset depicts the trajectory of the effective coupling $\tilde{g}(t) = \sqrt{2}g\langle a(t)\rangle$ in the complex plane due to the time evolution of the microwave amplitude. The phase-space orbit (black line) is numerically simulated from equation (4), while the limit cycle (green line) is an analytical approximation (see the appendix for more details).

For the choice of the other parameters, we focus on two sets of parameters corresponding to two completely different systems: an optical cavity with a moving mirror and a superconducting wave guide coupled to a mechanical resonator. The parameters are chosen according to realistic experimental settings; see, e.g. [5] (opto-mechanical system) and [9] (electro-mechanical system). Figures 3 and 4 show that, in both experimental scenarios, entanglement can significantly be increased by an appropriate modulation of the driving field.

7. Summary

In this paper, we have shown how time-modulation can significantly enhance the maximum degree of entanglement. Triggered by the time-modulated driving, the mode of the electromechanical field as well as the mechanical mode start 'rotating around each other' in a complex fashion, giving rise to increased degrees of entanglement. The dependence on frequencies of the additional modulation is intricate, with resonances greatly improving the amount of entanglement that can be reached. The ideas presented here could be particularly beneficial for preparing systems in entangled states in the first place, in scenarios where the parameters are such that the states prepared are close to the boundary to entangled states, but where this boundary is otherwise not yet quite reachable with the present technology. At the same time, such ideas are expected to be useful in metrological applications whenever high degrees of entanglement are needed.

Acknowledgments

We thank the EU (MINOS, COMPAS, QESSENCE) and the BMBF (QuOReP) for support.

Appendix

In this appendix, we derive analytical formulas for the asymptotic solutions of the classical system of dynamical equation (4). A crucial assumption for the following procedure is that it is possible to expand the solutions in powers of the coupling constant g

$$\langle O\rangle(t) = \sum_{j=0}^{\infty} O_j(t) g^j, \tag{A.1}$$

where $O = a, p, q$. This is justified only if the system is far away from multi-stabilities and the radiation pressure coupling can be treated in a perturbative way. A very important feature of the set of equation (4) is that they contain only two nonlinear terms and those terms are proportional to the coupling parameter g. This implies that, if we use the ansatz (A.1), each function O_j will be a solution of *linear* differential equation with time dependent parameters depending on the previous solution $O_{j-1}(t)$. Since $E(t) = E(t+\tau)$, from a recursive application of Floquet's theorem, follows that stable solutions will converge to periodic limit cycles having the same periodicity of driving: $\langle O(t)\rangle = \langle O(t+\tau)\rangle$. One can exploit this property and perform a double expansion in powers of g and in terms of Fourier components

$$\langle O\rangle(t) = \sum_{j=0}^{\infty} \sum_{n=-\infty}^{\infty} O_{n,j} \mathrm{e}^{in\Omega t} g^j, \tag{A.2}$$

where n are integers and $\Omega = 2\pi/\tau$. A similar Fourier series can be written for the periodic driving field,

$$E(t) = \sum_{n=-\infty}^{\infty} E_{\mathrm{N}} \mathrm{e}^{\mathrm{i}n\Omega t}. \tag{A.3}$$

The coefficients $O_{n,j}$ can be found by direct substitution in equation (4). They are completely determined by the following set of recursive relations:

$$q_{n,0} = p_{n,0} = 0, \quad a_{n,0} = \frac{E_{-n}}{\kappa + \mathrm{i}(\Delta + n\Omega)}, \tag{A.4}$$

corresponding to the 0-order perturbation with respect to g, and

$$p_{n,j} = \frac{\mathrm{i}n\Omega}{\omega_{\mathrm{m}}} q_{n,j}, \tag{A.5}$$

$$q_{n,j} = \omega_{\mathrm{m}} \sum_{k=0}^{j-1} \sum_{m=-\infty}^{\infty} \frac{a^*_{m,k}\, a_{n+m,j-k-1}}{\omega_{\mathrm{m}}^2 - n\Omega^2 + \mathrm{i}\gamma_{\mathrm{m}} n\Omega}, \tag{A.6}$$

$$a_{n,j} = \mathrm{i} \sum_{k=0}^{j-1} \sum_{m=-\infty}^{\infty} \frac{a_{m,k} q_{n-m,j-k-1}}{\kappa + \mathrm{i}(\Delta + n\Omega)}, \tag{A.7}$$

giving all the j-order coefficients in a recursive way. For all the examples analyzed in this paper, we truncated the analytical solutions up to $j \leqslant 3$ and $|n| \leqslant 2$. This level of approximation is already high enough to reproduce the exact numerical solutions well.

References

[1] Gigan S, Böhm H R, Paternostro M, Blaser F, Langer G, Hertzberg J B, Schwab K, Baeuerle D, Aspelmeyer M and Zeilinger A 2006 *Nature* **444** 67
[2] Arcizet O, Cohadon P-F, Briant T, Pinard M and Heidmann A 2006 *Nature* **444** 71
[3] Kleckner D and Bouwmeester D 2006 *Nature* **444** 75
[4] Schliesser A, Del'Haye P, Nooshi N, Vahala K J and Kippenberg T J 2006 *Phys. Rev. Lett.* **97** 243905
[5] Gröblacher S, Hammerer K, Vanner M R and Aspelmeyer M 2009 *Nature* **460** 724
[6] Riviere R, Deleglise S, Weis S, Gavartin E, Arcizet O, Schliesser A and Kippenberg T J 2011 *Phys. Rev.* A **83** 063835
[7] Chan J, Mayer Alegre T P, Safavi-Naeini A H, Hill J T, Krause A, Groeblacher S, Aspelmeyer M and Painter O 2011 *Nature* **478** 89
[8] Teufel J D, Harlow J W, Regal C A and Lehnert K W 2008 *Phys. Rev. Lett.* **101** 197203
[9] Teufel J D, Donner T, Li D, Harlow J H, Allman M S, Cicak K, Sirois A J, Whittaker J D, Lehnert K W and Simmonds R W 2011 *Nature* **475** 359
[10] Rocheleau T, Ndukum T, Macklin C, Hertzberg J B, Clerk A A and Schwab K C 2010 *Nature* **463** 72
[11] LaHaye M D, Buu O, Camarota B and Schwab K C 2004 *Science* **304** 74
[12] Knobel R G and Cleland A N 2003 *Nature* **424** 291
[13] Connell A D O *et al* 2010 *Nature* **464** 697
[14] Vitali D, Tombesi P, Woolley M J, Doherty A C and Milburn G J 2007 *Phys. Rev.* A **76** 042336
[15] Schwab K C and Roukes M L 2005 *Phys. Today* **58** 36
[16] Marquardt F and Girvin S M 2009 *Physics* **2** 40
[17] Aspelmeyer M 2010 *Nature* **464** 685

[18] Paternostro M, Vitali D, Gigan S, Kim M S, Brukner C, Eisert J and Aspelmeyer M 2007 *Phys. Rev. Lett.* **99** 250401
[19] Vitali D, Gigan S, Ferreira A, Böhm H R, Tombesi P, Guerreiro A, Vedral V, Zeilinger A and Aspelmeyer M 2007 *Phys. Rev. Lett.* **98** 030405
[20] Eisert J, Plenio M B, Bose S and Hartley J 2004 *Phys. Rev. Lett.* **93** 190402
[21] Mari A and Eisert J 2009 *Phys. Rev. Lett.* **103** 213603
[22] Woolley M J, Doherty A C, Milburn G J and Schwab K C 2008 *Phys. Rev.* A **78** 062303
[23] Clerk A A, Marquardt F and Jacobs K 2008 *New J. Phys.* **10** 095010
[24] Marquardt F, Chen J P, Clerk A A and Girvin S M 2007 *Phys. Rev. Lett.* **99** 093902
[25] Dobrindt J M, Wilson-Rae I and Kippenberg T J 2008 *Phys. Rev. Lett.* **101** 263602
[26] Eisert J 2001 *PhD Thesis* University of Potsdam (arXiv:quant-ph/0610253)
Eisert J and Plenio M B 1999 *J. Mod. Opt.* **46** 145
[27] Vidal G and Werner R F 2002 *Phys. Rev.* A **65** 032314
[28] Plenio M B 2005 *Phys. Rev. Lett.* **95** 090503
[29] Genes C, Mari A, Vitali D and Tombesi P 2009 *Adv. At. Mol. Opt. Phys.* **57** 33-86
[30] Tian L, Allman M S and Simmonds R W 2008 *New J. Phys.* **10** 115001